

## EPR Study of Gd<sup>3+</sup> Ions in $\beta$ -Alumina Single Crystals

J. ANTOINE, D. VIVIEN,\* J. THÉRY, AND R. COLLONGUES

*Laboratoire de Chimie Appliquée de l'Etat Solide (ERA 387), ENSCP, 11, rue Pierre et Marie Curie, 75231 Paris Cedex 05, France*

AND

J. LIVAGE

*Laboratoire de Spectrochimie du Solide (ERA 387), Université Pierre et Marie Curie, 4, place Jussieu, 75230 Paris Cedex 05, France*

Received December 14, 1976; in revised form March 11, 1977

Single crystals of  $\beta$ -alumina doped with Gd<sup>3+</sup> have been obtained by high-frequency induction melting of a NaAlO<sub>2</sub>-Al<sub>2</sub>O<sub>3</sub> mixture and slow cooling, followed by a Gd<sup>3+</sup>-Na<sup>+</sup> exchange in molten GdCl<sub>3</sub>. In these crystals, Gd<sup>3+</sup> occupies only one out of the several possible sites, in the spinel block and not in the conduction plane (which could be anticipated from the ionic radius of the ion). The EPR data can be described by a spin Hamiltonian which includes trigonal terms. The  $b_2^0$  value is close to 0.08 cm<sup>-1</sup>. These results suggest a localization of the ion either in the 4f-layer tetrahedra, or in an interstitial site. The second possibility, which is consistent with charge compensation (due to nonstoichiometry in  $\beta$ -alumina) by interstitial oxygen ions seems more likely.

### 1. Introduction

During the last 10 years,  $\beta$ -alumina has received a great deal of attention because of its very high ionic conductivity (1). This property allows it to be used as a solid electrolyte in high-energy density, rechargeable batteries.

$\beta$ -alumina is a sodium aluminate whose hexagonal structure (space group  $P6_3/mmc$ ) consists of spinel-like blocks with aluminium ions in both tetrahedral and octahedral interstices separated by mirror planes containing the sodium ions (2). The ionic conductivity of  $\beta$ -alumina, due to the migration of these sodium ions, strongly depends upon the impurity content of the material (3). In order to elucidate the mechanism by which the foreign ions act on the properties of  $\beta$ -alumina, it is necessary to know in which site of the structure they are located. Previous studies by electron paramagnetic resonance (EPR) and uv-visible

spectroscopy have shown that in  $\beta$ -alumina, Cr<sup>3+</sup> substitutes Al<sup>3+</sup> at the octahedral sites located in the spinel blocks (7) whereas Mn<sup>2+</sup> (4) and Cu<sup>2+</sup> (5, 6) can occupy several sites both in the spinel blocks and in the conduction planes. We found it of interest to study a case wherein the doping ion is confined in the conduction plane. This is what would be anticipated for Gd<sup>3+</sup> whose ionic radius (0.102 nm) is comparable to that of Na<sup>+</sup> (0.095 nm), both ions being larger than Al<sup>3+</sup> (0.050 nm).

In this work we present some EPR results obtained with Gd<sup>3+</sup>-doped  $\beta$ -alumina.

### 2. Experimental Procedure

Single crystals of  $\beta$ -alumina were obtained by slow cooling of a molten mixture containing  $\alpha$ -alumina and sodium aluminate NaAlO<sub>2</sub> in appropriate proportions (4). The faces of the clear thin plates extracted from the fusion-cast block are parallel to the conduction planes

\* To whom correspondence should be addressed.

( $aa^*$ ).<sup>1</sup> X-ray diffraction techniques confirm that they are good single crystals.

Various attempts to introduce the  $Gd^{3+}$  doping ions (as  $Gd_2O_3$ ) at the molten stage were unsuccessful. No  $Gd^{3+}$  EPR signals could ever be detected in the small crystals obtained after cooling. Consequently  $Na^+$  ions were substituted by  $Gd^{3+}$  in pure  $\beta$ -alumina single crystals by ionic exchange in molten  $GdCl_3$  following the usual procedure (8); the reaction was carried out under HCl atmosphere in order to prevent the formation of gadolinium oxychloride during the dehydration of commercial hydrated gadolinium trichloride.

The X-band (10 GHz) EPR spectrometer used was a JEOL ME3X, whose field has been calibrated with an accuracy of 0.2 mT by means of a variable frequency NMR device using proton and lithium resonance. The microwave radiation frequency was measured with an accuracy of 1 MHz by means of a tunable resonant cavity. Unless specified, spectra were obtained at a temperature of 296°K.

### 3. Experimental Results

When the static magnetic induction vector  $B_0$  has a general orientation with respect to the crystal axes, the EPR spectrum is rather complicated. However, the signals collapse into a few well-defined lines, which exhibit their highest intensity when the field is parallel or perpendicular to the  $c$  axis (Fig. 1); the distance between the extreme lines is maximum when  $B_0$  is parallel to  $c$ , while the spectrum is isotropic in the ( $aa^*$ ) plane. The spectra do not vary with temperature in the interval of 150 to 300°K. The linewidth ranges from 0.7 to 3 mT; this prevents the resolution of a hyperfine structure due to the two isotopes  $^{155}Gd$  and  $^{157}Gd$  ( $I = \frac{3}{2}$ ) which generally give hyperfine constants of about 0.5 mT (9). Figure 2 gives the angular variation of the spectrum according to the angle between the magnetic field and the  $c$  axis, in the ( $ca$ ) and ( $ca^*$ ) planes.

Some lines that could not be followed more

<sup>1</sup> The (01.0), ( $\bar{1}$ 2.0), (00.1) crystallographic planes are called ( $ca$ ), ( $ca^*$ ), ( $aa^*$ ), respectively, referring to the principal directions they contain.

than a few degrees (too anisotropic, broad, and weak, or hidden by other lines) were omitted from the graphs of Fig. 2. The main difference between the ( $ca$ ) and ( $ca^*$ ) planes comes from the splitting occurring for some lines in the ( $ca^*$ ) plane, when  $B_0$  is not parallel to the  $c$  axis, or the ( $aa^*$ ) plane. Furthermore, for a given angle, the lines observed in the ( $ca$ ) plane are situated exactly in the middle of the two corresponding ones in the ( $ca^*$ ) plane.

In contrast with what has been observed for  $Cu^{2+}$  (5) or  $Mn^{2+}$  (4), the spectra of the crystals do not depend upon the conditions of ionic exchange, for periods ranging from 3 min to 1 hr and temperatures from 950 to 1250°K. For longer periods and higher temperatures, a broad and strong line due to magnetically interacting  $Gd^{3+}$  ions develops in the  $g = 2$  region, overlapping the previously described lines. Therefore spectra have not been investigated under these conditions. This broad line begins to appear already in the spectra depicted Fig. 1.

The spectrum is not modified by annealing the doped crystals at 900–1300°K for periods of up to 12 days, or by a treatment in molten sodium iodide at 900°K for 2 days. Finally, pure crystals which have been refluxed for 3 weeks in a concentrated aqueous solution of  $GdCl_3$  show the same  $Gd^{3+}$  spectrum. But in that case, the lines are very weak.

### 4. Attribution of the EPR Spectrum

Chemical experiments and EPR data indicate that  $Gd^{3+}$  occupy only one kind of site in  $\beta$ -alumina. This site exhibits an axial symmetry, the  $oz$  axis being the  $c$  direction of the crystal.

To begin with, we have used the approximate spin Hamiltonian adapted to a  $^8S_{7/2}$   $Gd^{3+}$  ion in axial symmetry (10):

$$\hat{H}_s = \beta(B.g.S) + (1/3)b_2^0 O_2^0 + (1/60)b_4^0 O_4^0 + (1/1260)b_6^0 O_6^0 + (1/1260)b_6^6 O_6^6$$

The term in  $O_6^6$  goes as  $\cos 6\phi$  (11), where  $\phi$  is the angle between  $ox$  (taken as the reference axis in the ( $aa^*$ ) plane), and the ( $B_0$ ,  $oz$ ) plane. This introduces a small angular dependence of the position of the resonant lines, the periodicity of which is 60° (12) when  $B_0$  is

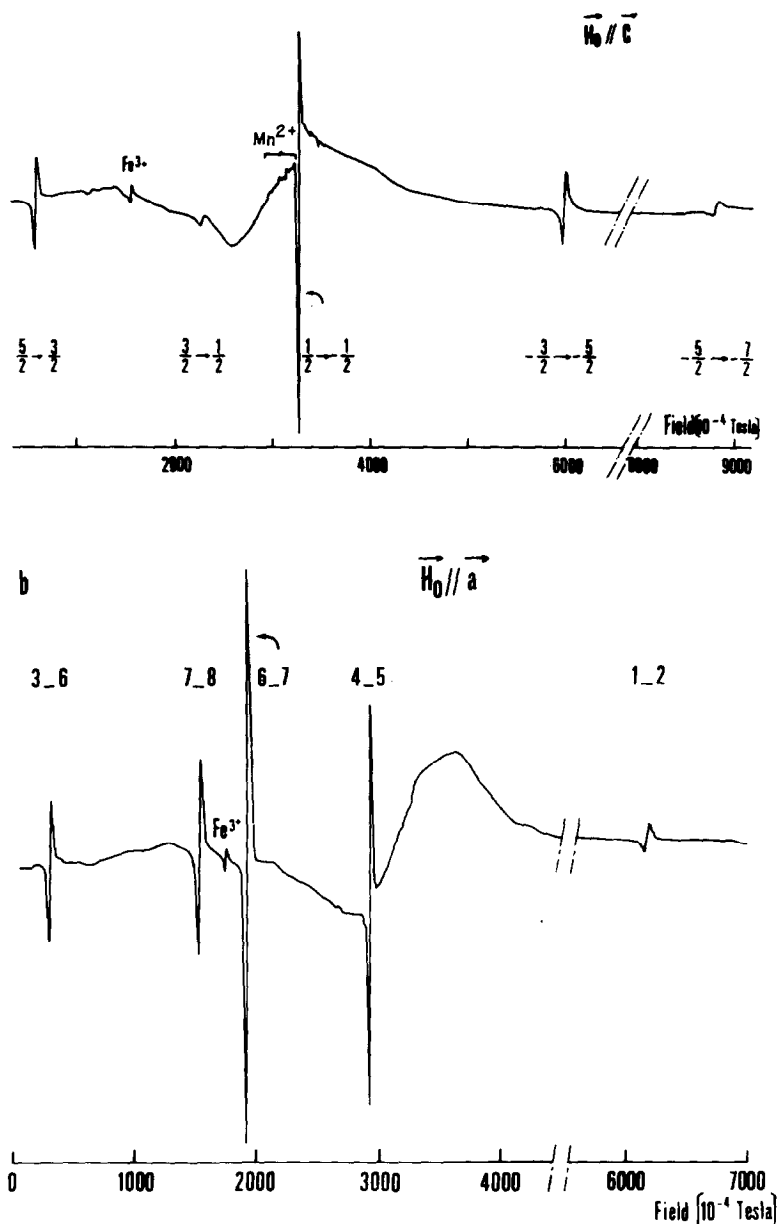


FIG. 1. EPR spectrum of  $Gd^{3+}$  in  $\beta$ -alumina ( $X$  band), (a) the magnetic field is parallel to the  $c$  axis of the crystal, (b) the magnetic field is parallel to the  $a$  axis of the crystal. Transitions are labeled either by the spin value  $M_s$ , or by the number (in order of decreasing energy) of the levels between which they occur (see text). A few extra lines coming from  $Fe^{3+}$  or  $Mn^{2+}$  impurities can be recognized on the two spectra. From the intensity of the  $\frac{1}{2} \rightarrow -\frac{1}{2}$  transition for  $B_0 \parallel c$ , it can be estimated that in the crystal, the  $Gd^{3+}$  concentration responsible of the narrow lines spectra was lower than 0.05% per  $Al^{3+}$  ion.

rotated in the  $(aa^*)$  plane. Experimentally, the positions of the lines in the  $(aa^*)$  plane do not vary with the angle  $\phi$ . This shows (11, 12)

that, to the accuracy of the measurements (which is limited to about 1 mT, because of uncertainty in the magnetic induction values,

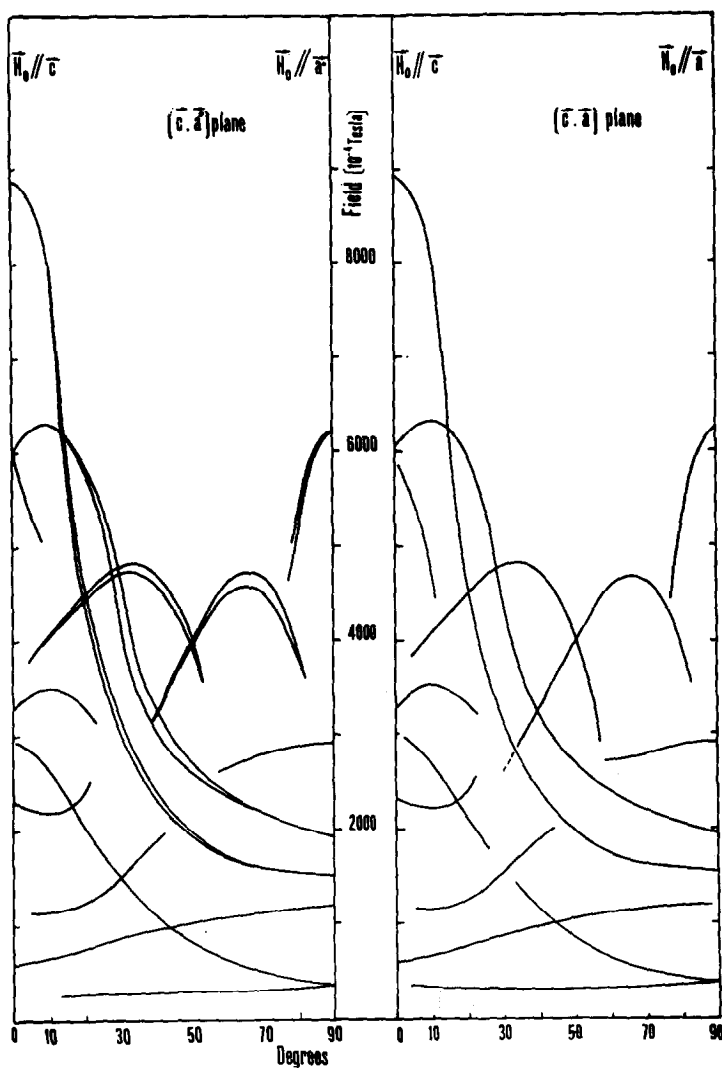


FIG. 2. Experimental angular variation of the EPR spectrum, according to the angle between the magnetic field, and the  $c$  axis of the crystal, in the  $(ca^*)$  and  $(ca)$  planes.

crystal orientation, and because of linewidths), the  $b_6^6$  parameter can be neglected. Consequently, the term in  $b_6^6 O_6^6$  is henceforth ignored in the spin Hamiltonian.

Using the experimental field values for the  $z$  direction, and formulas deduced from perturbation theory (10) one can obtain approximate values of the main zero field terms:

$$b_2^0 = 0.08 \text{ cm}^{-1}, \quad b_4^0 = 0.002 \text{ cm}^{-1}.$$

These values are used as starting parameters in a least-squares-fitting computer program

(13) which carries out the exact diagonalization of the energy matrix.

Regarding the splitting of the lines in the  $(ca^*)$  plane (Fig. 2) we notice that similar behavior has been observed for  $\text{Gd}^{3+}$  in  $\alpha$ -alumina where it substitutes  $\text{Al}^{3+}$  in  $C_3$ -symmetry sites (11). This splitting has been explained by the influence, in the spin Hamiltonian, of the trigonal terms  $O_4^3$  and  $O_6^3$  which go, respectively, as  $z \cos 3\phi$  and  $z^3 \cos 3\phi$ .

In our case it was found, by the least-squares

adjustment of the zero field parameters on the  $z$  axis transitions, that the mean deviation<sup>2</sup> can be significantly lowered by introducing the trigonal terms  $\frac{1}{3}b_4^3 O_4^3 + \frac{1}{36}b_6^3 O_6^3$  in the spin Hamiltonian. This confirms that Gd<sup>3+</sup> in  $\beta$ -alumina undergoes a trigonal crystal field for which associated point symmetry should be either  $C_3$  or  $C_{3i}$  ( $S_6$ ),  $C_{3v}$ ,  $D_3$ ,  $D_{3d}$  (10).

We emphasized in the preceding section that the single line observed in the ( $ca$ ) plane, for a particular transition and a given angle, lies in the middle of the corresponding doublet in the ( $ca^*$ ) plane. This can be interpreted by assuming that Gd<sup>3+</sup> occupies different sites having the same  $oz$  axis, but whose  $ox$  axis are not coincident. The sites should be such that when the field lies in the ( $ca$ ) plane, contribution from the trigonal term of  $\hat{H}_s$  is zero:  $\cos 3\phi = 0$ ,  $\phi = 30$  or  $90^\circ$ ; while in the ( $ca^*$ ) plane, contributions from these terms are  $\cos 3\phi = -1$ ,  $\phi = 60^\circ$  or  $\cos 3\phi = 1$ ,  $\phi = 0^\circ$ . It

<sup>2</sup> The mean deviation of the fit is defined as  $(1/N)[\sum_{j=1, N} (|\Delta E_j| - hv)^2]^{1/2}$ , where  $hv$  is the energy of the microwave radiation,  $\Delta E_j$  is the energy difference between levels participating to the  $J$ th resonance, and  $N$  is the number of experimental field transition included in the fit.

follows that the  $ox$  axes are along the  $a^*$  directions.

Then we have used the full spin Hamiltonian and the exact diagonalization program to find the best set of parameters describing the spectra for the  $c$  direction, ( $aa^*$ ) plane, and several intermediate orientations of the field. Some difficulties occur from the fact that the  $b_2^0$  parameter is not small compared to the quantum of energy at the  $X$  band. This leads to a divergence of the least-squares refinement if all the spin Hamiltonian parameters are allowed to vary simultaneously (7). Consequently, the zero field parameters were first varied,  $g_{\parallel}$  and  $g_{\perp}$  being set to 2.01 (the value deduced from the position of the  $\frac{1}{2} \rightarrow -\frac{1}{2}$  transition, for  $\mathbf{B}_0 \parallel oz$ ). Then  $g_{\parallel}$  and  $g_{\perp}$  were refined, and a new variation of the  $b_n^m$  parameters, at constant  $g_{\parallel}$  and  $g_{\perp}$ , were performed.

The spin Hamiltonian parameters obtained are represented in Table I.

From Table I, it can be noticed that  $g_{\perp}$  has an abnormally low value which we are unable to account for at present. On the other hand,  $b_2^0$  has the expected magnitude.

Table II gives the field values of the experi-

TABLE I  
SPIN HAMILTONIAN PARAMETERS FOR Gd<sup>3+</sup> IN  $\beta$ -ALUMINA<sup>a</sup>

$b_2^0$	$b_4^0$	$b_6^0$	$b_4^3$	$b_6^3$	$g_{\parallel}$	$g_{\perp}$
0.0779	0.0005	0.0041	0.0019	0.0025	1.992	1.548

<sup>a</sup> The non-Zeeman parameters are in  $\text{cm}^{-1}$ . The mean deviation (see footnote 2) of the fit is  $0.0046 \text{ cm}^{-1}$ . The errors on all the  $b_n^m$  parameters are identical and are estimated at  $0.0015 \text{ cm}^{-1}$ . The errors on the  $g$  values are 0.01.

TABLE II  
EXPERIMENTAL FIELD VALUES AND ASSIGNMENT FOR THE Gd<sup>3+</sup>:  $\beta$ -ALUMINA EPR SPECTRUM<sup>a</sup>

	$\mathbf{B}_0 \parallel c$				
Experimental field (T)	0.0588	0.2303	0.3283	0.5987	0.8874
Assignment	$\frac{5}{2} \frac{3}{2}$	$\frac{3}{2} \frac{1}{2}$	$\frac{1}{2} -\frac{1}{2}$	$-\frac{3}{2} -\frac{5}{2}$	$-\frac{5}{2} -\frac{7}{2}$
	$\mathbf{B}_0 \perp c$				
Experimental field (T)	0.0306	0.1528	0.1923	0.2911	0.6212
Assignment	3-6	7-8	6-7	4-5	1-2

<sup>a</sup> Error:  $\pm 0.5 \text{ mT}$ ; frequency:  $9225.7 \pm 0.5 \text{ MHz}$ .

mental lines and the energy levels between which the transitions occur. Due to the mixing of the spin wavefunctions the levels are numbered 1, 2, ..., 8 in the order of decreasing energy (instead of the  $M_s$  value) for  $B_0$  perpendicular to  $c$ .

The assignment is based on an exact diagonalization of the spin-Hamiltonian matrix, using the zero field parameters of Table I.

### 5. Localization of $Gd^{3+}$ in the Structure

Chemical experiments (see Sect. 3) indicate that the  $Gd^{3+}$  ions are in the spinel blocks rather than in the conduction planes. Otherwise, annealing of the crystal would have probably induced the migration of  $Gd^{3+}$  toward some sites of the spinel block, as observed for  $Mn^{2+}$  and  $Cu^{2+}$  (5). At least, treatment of the  $Gd^{3+}$ -doped crystal in molten NaI should have removed all the gadolinium ions from the conduction planes (4). This result is quite surprising because one should have expected to find the gadolinium ions in the conduction planes (see Sect. 1). Localization of  $Gd^{3+}$  in the spinel blocks could be related to the fact that there are no  $\beta$ -alumina-type compounds in the  $Gd_2O_3$ - $Al_2O_3$  phase diagram (while such structures have been observed with the largest rare earth ions  $Nd^{3+}$  and  $La^{3+}$  (14)). This could also explain why various attempts to prepare doped crystals (see Sect. 2) by introducing  $Gd_2O_3$  in molten  $\beta$ -alumina have been unsuccessful.

Among the various crystallographic positions allowed in the space group  $P6_3/mmc$ , for an ion in the spinel blocks, only the  $4e$  and  $4f$  (in Wyckoff notation) have a point symmetry (actually  $C_{3v}$ ) consistent with the EPR results (see Sect. 4). If we assume that  $Gd^{3+}$  substitutes  $Al^{3+}$  on its own crystallographic positions, we are left with two kinds of  $4f$  tetrahedral sites (Fig. 3). The  $4f$ -block tetrahedra positions situated in the middle of the spinel block (Fig. 3) seem very unlikely owing to the fact that  $Gd^{3+}$  reaches its site in the structure very easily during the doping process (see Sect. 3). The only sites which remain are the  $4f$ -layer tetrahedra which are very close to the conduction plane (Fig. 3).

If  $Gd^{3+}$  occupies these sites, this could indi-

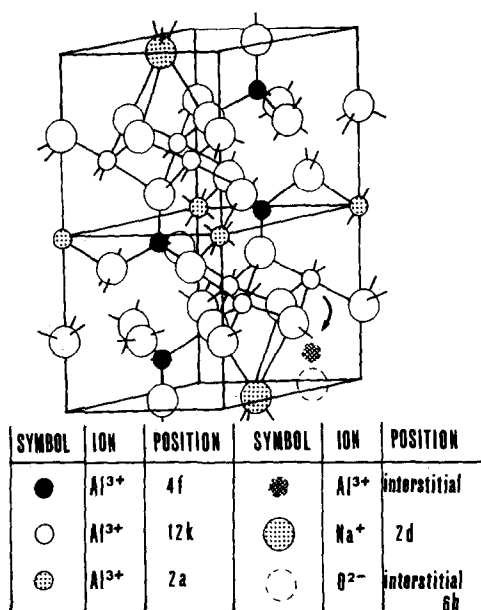


FIG. 3. Partial view of the unit cell of  $\beta$ -alumina showing one spinel-like block delimited by two conduction planes. The black circles correspond to the  $4f$ -block or -layer tetrahedra. The circle with crossing lines, at the bottom right of the spinel block, corresponds to aluminum ions in a Frenkel defect, when associated with an aluminum vacancy at the  $12k$  position, just above it.

cate that the charge compensation needed by the excess of sodium ions (see Sect. 1) takes place by the creation of aluminium vacancies in these  $4f$ -layer tetrahedra positions.

However, there is another possibility which is consistent with electrical compensation by interstitial oxygen ions in the conduction planes. In this mechanism, the  $Gd^{3+}$  ions would occupy the same position as  $Al^{3+}$  in the Frenkel defect that has already been observed in sodium (15) and potassium (16)  $\beta$ -alumina (Fig. 3). But of course, there will be no associated aluminum vacancies in the  $12k$  positions. These two possibilities correspond to sites which for their first neighbors have the same geometry. So it is difficult to come to a firm conclusion on the basis of the EPR data. However, recent results obtained in our laboratory, either on  $\beta$ -alumina (3), or its isomorphous sodium gallate (17) are in favor of an in-

terstitial oxygen mechanism. Consequently, the second possibility seems to be more likely.

### References

1. J. T. KUMMER, *Progr. Solid State Chem.* **7**, 141 (1972) (Pergamon).
2. C. R. PETERS, M. BETTMAN, J. W. MOORE, AND M. D. GLUCK, *Acta Crystallogr. B* **27**, 1826 (1971).
3. J. P. BOILOT AND J. THERY, *Mater. Res. Bull.* **11**, 407 (1976).
4. J. ANTOINE, D. VIVIEN, J. LIVAGE, J. THERY, AND R. COLLONGUES, *Mater. Res. Bull.* **10**, 865 (1975).
5. D. VIVIEN, J. ANTOINE, D. GOURIER, J. THERY, J. LIVAGE, AND R. COLLONGUES, in "Colloque International du C.N.R.S. sur la spectroscopie des éléments de transition et des éléments lourds dans les solides, Lyon, Juin 1976," CNRS special publication, 1977, in press.
6. D. VIVIEN, J. ANTOINE, AND J. LIVAGE, ESR Symposium NIJMEGEN, August (1976), The Netherlands.
7. J. ANTOINE, Ph.D. Thesis, Paris, 1976.
8. Y. F. YU YAO AND J. T. KUMMER, *J. Inorg. Nucl. Chem.* **29**, 2453 (1967).
9. C. F. HEMPSTEAD AND K. D. BOWERS, *Phys. Rev.* **118**, 131 (1960).
10. H. A. BUCKMASTER AND Y. H. SHING, *Phys. Status Solidi (a)* **12**, 325 (1972).
11. S. GESCHWIND AND J. P. REMEKA, *Phys. Rev.* **122**, 757 (1961).
12. D. VIVIEN, A. KAHN, A. M. LEJUS AND J. LIVAGE, *Phys. Status Solidi (b)* **73**, 593 (1976); W. LOW, A. ZUSMAN, *Phys. Rev.* **130**, 144 (1963).
13. D. VIVIEN AND J. F. GIBSON, *J. Chem. Soc. Faraday II* **71** (1640) (1975).
14. I. A. BUNDAR AND H. A. TOROPOV, *Izv. Acad. Nauk SSSR Ser. Khim* **2**, 212 (1966).
15. W. L. ROTH AND F. REIDINGER, General Electric Company, Technical Information Series Report n°74, CDR 054, March (1974).
16. G. COLLIN, J. P. BOILOT, A. KAHN, J. THERY, AND R. COMES, *J. Solid State Chem.* **21**, 283 (1977).
17. A. KAHN, J. P. BOILOT AND J. THERY, *Mater. Res. Bull.* **11**, 397 (1976).